Title: Upregulation of Thrombin/Matrix Metalloproteinase-1/Protease-activated Receptor-1 chain in Proliferative Diabetic Retinopathy

Short title: Thrombin/MMP-1/PAR1 in diabetic retinopathy

Authors: Ahmed M. Abu El-Asrar[1,2] MD, PhD; Kaiser Alam[1], PhD; Mohd Imtiaz Nawaz[1], MSc; Ghulam Mohammad[1], PhD; Kathleen Van den Eynde[3], MSc; Mohammad Mairaj Siddiquei[1], MSc; Ahmed Mousa, PhD[1]; Gert De Hertogh[3], MD, PhD; Ghislain Opdenakker[4], MD, PhD

Affiliations:

[1]Department of Ophthalmology, College of Medicine, King Saud University, Riyadh, Saudi Arabia.

[2]Dr. Nasser Al-Rashid Research Chair in Ophthalmology, Riyadh, Saudi Arabia

[3]Laboratory of Histochemistry and Cytochemistry, University of Leuven, KU Leuven, Belgium

[4]Rega Institute for Medical Research, Department of Microbiology and Immunology, University of Leuven, KU Leuven, Belgium.

Correspondence to:

Ahmed M. Abu El-Asrar, MD, PhD., Department of Ophthalmology

King Abdulaziz University Hospital, Old Airport Road, P.O. Box 245,

Riyadh 11411, Saudi Arabia.

Tel: 966-11-4775723 Fax: 966-11-4775724

E-mail: abuasrar@KSU.edu.sa / abuelasrar@yahoo.com

Abstract

Purpose: Selective proteolytic activation of protease-activated receptor-1 (PAR1) by thrombin and matrix metalloproteinase-1 (MMP-1) plays a central role in enhancing angiogenesis. We investigated the expression levels of thrombin, MMP-1 and PAR1 and correlated these levels with vascular endothelial growth factor (VEGF) in proliferative diabetic retinopathy (PDR). In addition, we examined the expression of PAR1 and thrombin in the retinas of diabetic rats and PAR1 in human retinal microvascular endothelial cells (HRMEC) following exposure to high-glucose, the proinflammatory cytokines interleukin-1β (IL-1β) and tumor necrosis factor-α (TNF-α) and the hypoxia mimetic agent cobalt chloride ($CoCl_2$).

Methods: Vitreous samples from 32 PDR and 23 nondiabetic patients, epiretinal membranes from 10 patients with PDR, retinas of rats and HRMEC were studied by enzyme-linked immunosorbent assay (ELISA), immunohistochemistry and Western blot analysis. An assay for *in vitro* cell migration angiogenesis was performed in HRMEC.

Results: In epiretinal membranes, PAR1 was expressed in vascular endothelial cells, CD45-expressing leukocytes and myofibroblasts. ELISA and Western blot assays revealed significant increases in the expression levels of thrombin, MMP-1 and VEGF in vitreous samples from PDR patients compared to nondiabetic controls. Significant positive correlations were found between the levels of VEGF and the levels of thrombin ($r=0.41$; $p=0.006$) and MMP-1 ($r=0.66$; $p<0.0001$). Significant increases of cleaved PAR1 (approximately 50 kDa) and the proteolytically active thrombin (approximately 50 kDa) were detected in rat retinas after induction of diabetes. The proinflammatory cytokines IL-1β and TNF-α, but not high-glucose and $CoCl_2$, induced upregulation of cleaved PAR1 (approximately 30 kDa) in HRMEC. In addition, thrombin and MMP-1 induced VEGF in HRMEC and vorapaxar, a PAR1 inhibitor, inhibited thrombin-induced migration in HRMEC.

Conclusions: Interactions between thrombin, MMP-1, PAR1 and VEGF might facilitate angiogenesis in PDR.

Key words: proliferative diabetic retinopathy; angiogenesis; protease-activated receptor-1; thrombin; matrix metalloproteinase-1

Introduction

Ischemia-induced angiogenesis, a process by which new blood vessels are formed from pre-existing ones, is a hallmark feature of proliferative diabetic retinopathy (PDR) and is a critical step in the progression of the disease. This process takes place as a consequence of an angiogenic switch, which allows the recruitment of blood vessels from neighboring tissues [1-3]. Vascular endothelial growth factor (VEGF) is the major angiogenic factor in PDR that promotes neovascularization and vascular leakage [4]. In addition, chronic, low-grade subclinical inflammation is responsible for many of the vascular lesions in diabetic retinopathy [5-7]. The causal relationship between inflammation and angiogenesis is now widely accepted [8]. An emerging issue in diabetic retinopathy research is the focus on the mechanistic link between chronic, low-grade inflammation and angiogenesis. Therapeutic regulation of angiogenesis is an attractive approach for the treatment of PDR [9]. To aid the progress of anti-angiogenic therapies, a more comprehensive understanding of molecules regulating angiogenesis in PDR is of value in order to identify additional therapeutic targets and to avoid potential detrimental side-effects.

Protease-activated receptor-1 (PAR1) is a G protein-coupled receptor. This receptor carries its own ligand, which remains silent until the serine protease thrombin and other proteases cleave at a specific site within the extracellular N-terminus exposing a new N-terminal-tethered ligand domain that binds and activates the cleaved receptor [10-12]. More recently, the zinc-dependent matrix metalloproteinase-1 (MMP-1) was identified as having the capacity to cleave and activate PAR1 [10-13]. Signal transduction initiated by PAR1 activation has many downstream consequences, leading to changes in cellular morphology, proliferation, migration, and adhesion [10]. It was recently shown that selective proteolytic activation of PAR1 by thrombin and MMP-1 plays a central role in enhancing both angiogenesis and tumor growth [10, 13-18]. In addition, activation of PAR1 leads to synthesis and secretion of functional VEGF protein and that PAR1-induced angiogenesis is mediated by VEGF [17].

Given the key roles of PAR1/ MMP-1/thrombin axis in angiogenesis, we investigated the hypothesis that this axis may be involved in the pathogenesis of PDR. To test this hypothesis, we investigated the expression of MMP-1, thrombin and PAR1 in the vitreous fluid and epiretinal fibrovascular membranes from patients with PDR and correlated MMP-1 and thrombin levels with the levels of the angiogenic factor VEGF. In addition, to corroborate a functional link between this axis and diabetes, we investigated the expression of PAR1 and thrombin in the retinas of diabetic rats and PAR1 in human retinal microvascular endothelial cells (HRMEC) following exposure to high-glucose to replicate hyperglycemia, to the proinflammatory cytokines interleukin-1β (IL-1β) and tumor necrosis factor-α (TNF-α) as a means to mimic inflammation and to the hypoxia-mimetic agent cobalt chloride ($CoCl_2$). Finally, we further examined whether vorapaxar (formerly known as SCH530348), a potent PAR1 receptor antagonist [19], blocked thrombin-induced migration in HRMEC.

Materials and Methods

Vitreous samples and epiretinal membranes specimens

Undiluted vitreous fluid samples (0.3 – 0.6 ml) were obtained from 32 patients with PDR during pars plana vitrectomy. The indications for vitrectomy were tractional retinal detachment, and/or nonclearing vitreous hemorrhage. The control group consisted of 23 patients who had undergone vitrectomy for the treatment of rhegmatogenous retinal detachment with no proliferative vitreoretinopathy. The duration of retinal detachment ranged from 2 to 11 days, with a mean of 5.9 ± 2.7 days. Controls were free from systemic disease. Vitreous samples were collected undiluted by manual suction into a syringe through the aspiration line of vitrectomy, before opening the infusion line. The samples were centrifuged (500 rpm for 10 min, 4°C) and the supernatants were aliquoted and frozen at -80°C until assay. Epiretinal fibrovascular membranes were obtained from 10 patients with PDR during pars plana vitrectomy for the repair of tractional retinal detachment. Membranes were fixed for 2 hours in 10% formalin solution and embedded in paraffin.

The study was conducted according to the tenets of the Declaration of Helsinki. All the patients were candidates for vitrectomy as a surgical procedure. All patients signed a preoperative informed written consent and approved the use of the excised epiretinal membranes and vitreous fluid for further analysis and clinical research. The study design and the protocol were approved by the Research Centre and Institutional Review Board of the College of Medicine, King Saud University.

Rat streptozotocin-induced diabetes model

All procedures with animals were performed in accordance with the ARVO statements for the use of animals in ophthalmic and vision research and were approved by the Institutional Animal Care and Use Committee of the College of Pharmacy, King Saud University. Adult male Sprague-Dawley rats, 8-9 weeks of age weighting in the range of 220-250 g were overnight fasted and streptozotocin (STZ) (65 mg/kg in 50 mM sodium citrate buffer, pH 4.5; Sigma, St. Louis, MO) was injected intraperitoneally. Equal volumes of citrate buffer were injected in control non-diabetic animals. Measurement of blood glucose concentrations and body weight were started 3 days after injection of STZ. Diabetes was confirmed by assaying the glucose concentration in blood taken from the tail vein. Rats with glucose levels >250 mg/dl were categorized as diabetic. After 4 weeks of diabetes, animals were anesthetized by intraperitoneal injection of an overdose of chloral hydrate and sacrificed by decapitation. Retinas were dissected, flash frozen and stored at -70^{0}C until use. Similarly, retinas were obtained from age-matched nondiabetic control rats.

Cell culture

Primary human retinal microvascular endothelial cells (HRMEC) were purchased from Cell Systems Corporation (Kirkland, Washington, USA) and maintained in complete serum free media (Cat. No. SF-4Z0-500, Cell System Corporation) supplemented with recombinant RocketFuel (Cat No. SF-4Z0-500, Cell System Corporation), CultureBoost (Cat. No. 4CB-500, Cell System Corporation) and antibiotics (Cat. No. 4Z0-643, Cell System Corporation) at 37°C in a humidified atmosphere with 5% CO_2. We used HRMEC cells only up to passage 8 for all the experiments. When HRMEC cells became ~80% confluent, cells were starved in minimal media (medium with antibiotics and 0.25% RocketFuel and without CultureBoost) overnight to eliminate any residual effects of growth factors. Following

starvation, HRMEC were either left untreated or treated either with 10 ng/ml of recombinant human (rh) IL-1β (Cat. No. 201-LB, R&D Systems, Minneapolis, MN), 30 ng/ml rh TNF-α (Cat. No. 210-TA, R&D Systems, Minneapolis, MN), rh IL-1β plus TNF-α, 1nM rh thrombin (Cat. No. 1773SE, R&D Systems), 5 nM rh MMP-1(Cat. No. ab39297, Abcam, Cambridge, UK) or 100 μM cobalt chloride ($CoCl_2$) (AVONCHEM limited, Macclesfield, Cheshire SK116PJ, United Kingdom) for 24 hours or with 30 mM glucose (Scharlau, Sentmenat, SPAIN) or 30 mM mannitol (Scharlau, Sentmenat, SPAIN) (as an osmotic control) for 72 hours. Wherever needed, cells were pre-treated for 30 minutes with the specific PAR1 inhibitor vorapaxar at a concentration of 10 μM (Cat. No. sc-394048 Santa Cruz Biotechnology Inc, Santa Cruz, CA). Each experiment was done at least three times with duplicate cell culture conditions.

Enzyme-linked immunosorbent assays

An enzyme-linked immunosorbent assay (ELISA) kit for human VEGF (Cat No: SVE00) was purchased from R&D Systems. ELISA kits for thrombin (Cat No: ab108909) and MMP-1 (Cat No: ab100603) were purchased from Abcam, Cambridge, UK. The thrombin ELISA kit recognizes both natural and recombinant human thrombin. The MMP-1 ELISA kit detects human pro and active forms. The minimum detection limits for the VEGF, thrombin and MMP-1 ELISA kits were 9 pg/mL, 0.3 ng/mL and 8 pg/mL, respectively. The ELISA plate readings were done using a Stat Fax-4200 microplate reader from Awareness Technology, Inc., Palm City, FL.

The quantification of human VEGF, Thrombin and MMP-1 in vitreous fluids was determined with the use of commercially available ELISAs in accordance with the manufacturer's instructions. For each ELISA, the undiluted standard served as the highest standard and calibrator diluents were used as the zero standard. Depending on the detection range for each ELISA kit, vitreous fluid samples were adequately diluted with calibrator diluents supplied with each ELISA kit.

For the measurement of VEGF and MMP-1, 100 μl of undiluted vitreous samples were used. For the measurement of thrombin, 100 μl of 4-fold diluted vitreous samples were analyzed. As instructed in the manuals, samples were incubated into each well of the ELISA plates. Antibodies against VEGF, thrombin and MMP-1 conjugated to horseradish peroxidase (HRP) were added to each well of the ELISA plates. After incubation, a substrate mix solution (1:1, hydrogen peroxide:tetramethylbenzidine) was added for color development. The reaction was stopped by the addition of 2N sulfuric acid (R & D Systems), and the optical density was read at 450 nm in a microplate reader. Each assay was performed in duplicate. Using the 4-parameter fit logistic (4-PL) curve equation, the actual concentration of each sample was calculated. For the diluted vitreous fluids, the correction read from the standard curve obtained using 4-PL was multiplied by the dilution factor to calculate the actual reading for each sample.

Western blot analysis for thrombin, MMP-1, PAR1 and VEGF

Retinas from diabetic and control rats were homogenized in Western blot lysis buffer (30 mM Tris-HCl; pH 7.5, 5 mM EDTA, 1% Triton X-100, 250 mM sucrose, 1 mM Sodium vanadate and protease inhibitor cocktail). The protease inhibitor used was "Complete without EDTA" (Roche, Mannheim, Germany). The homogenates were centrifuged at 14,000g for 15 minutes at 4°C and the supernatants were used for protein estimation and further analysis. HRMEC were lysed after harvest with RIPA buffer (50 mM Tris/HCl [pH 7.5], 150 mM

NaCl, 1% (v/v) Nonidet P40 (NP40), 0.5% Sodium deoxycholate, 0.1% SDS and protease inhibitor "Complete without EDTA" (Roche, Mannheim, Germany). Whole cell extracts from different treated groups were centrifuged at 12,000 ×g for 10 min at 4°C. The supernatants were collected and protein concentrations were measured with the use of DC protein assay kit (Bio-Rad Laboratories, Hercules, CA, USA). Equal amounts of protein (50 μg) were subjected to SDS-polyacrylamide gel (SDS-PAGE) electrophoresis in 8-10% gels and transferred onto nitrocellulose membranes (Bio-Rad Laboratories). To determine the expression levels of thrombin and MMP-1 in the vitreous samples, equal volumes (15 μl) of vitreous samples were boiled in Laemmli's sample buffer (1:1, v/v) under reducing conditions for 10 min and analyzed as described. Nonspecific binding sites were blocked (1.5 hours, room temperature) with 5 % non-fat milk made in Tris-buffered saline containing 0.1%Tween-20 (TBS-T)). Blots were then incubated at 4^0C overnight using the following primary antibodies; anti-thrombin (1:1000; ab-92621; Abcam), anti-MMP-1 (1:500; sc-30069; Santa Cruz Biotechnology Inc, Santa Cruz, CA), anti-PAR1 (1:1000, mab-3855, R&D Systems) and anti-VEGF (1:500, Cat. No. MAB293 R&D Systems). Three TBS-T washings (5 min each) were performed prior to respective secondary antibody treatment at room temperature for 1 hour. Finally, the immunodetection was performed with the use of chemiluminescense Western blotting luminol reagent (sc-2048; Santa Cruz Biotechnology Inc). Membranes were stripped and reprobed with β-actin-specific antibody (1:2000; sc-47778; Santa Cruz Biotechnology Inc) used as the lane-loading control. Bands were visualized with the use of a high-performance chemiluminescence machine (G: Box Chemi-XX8 from Syngene, Synoptic Ltd. Cambridge, UK), and the intensities were quantified by using GeneTools software (Syngene by Synoptic Ltd.).

In vitro migration assay

HRMEC were plated at 1×10^5 cells/well on 6-well culture plates and allowed to grow as described above till 80–90% confluency. Quiescence was induced by incubating the cells in minimal media overnight. Scratches were made with a sterile pipette tip and then cells were rinsed with PBS. Cells were either left untreated or treated either with 1nM thrombin or 5nM MMP-1 or with 10 μM vorapaxar for 30 minutes before addition of thrombin, and then cells were incubated for further 16 hours. Cell migration was monitored by visual examination using an inverted microscope (Olympus 1X 81). Analysis of migration was done using Image J software.

Immunohistochemical staining

For CD31, α-smooth muscle actin (α-SMA) and PAR1, antigen retrieval was performed by boiling the sections in citrate based buffer [pH 5.9 – 6.1] [BOND Epitope Retrieval Solution 1; Leica] for 10 minutes. For CD45 detection, antigen retrieval was performed by boiling the sections in Tris/EDTA buffer [pH 9] [BOND Epitope Retrieval Solution 2; Leica] for 20 minutes. Subsequently, the sections were incubated for 60 minutes with mouse monoclonal anti-CD31 (ready-to-use; clone JC70A; Dako, Glostrup, Denmark), mouse monoclonal anti-CD45 (ready-to-use; clones 2B11+PD7/26; Dako), mouse monoclonal anti-α-smooth muscle actin (ready-to-use; clone 1A4; Dako) and rabbit polyclonal anti-PAR1 antibody (1:200, APR-031, Alomone Labs, Jerusalem, Israel). Optimal working concentrations and incubation times for the antibodies were determined earlier in pilot experiments on sections from placenta and from patients with glioblastoma. The sections were then incubated for 20 minutes with a post primary IgG linker followed by an alkaline phosphatase conjugated polymer. The reaction product was visualized by incubation

for 15 minutes with the Fast Red chromogen, resulting in bright-red immunoreactive sites. The slides were then faintly counterstained with Mayer's hematoxylin [BOND Polymer Refine Red Detection Kit; Leica].

To identify the phenotype of cells expressing PAR1, sequential double immunohistochemistry was performed. The sections were incubated with the first primary antibody (anti-CD45) and subsequently treated with peroxidase conjugated secondary antibody. The sections were visualized with 3, 3'-diaminobenzidine tetrahydrochloride. Incubation of the second primary antibody (anti-PAR1) was followed by treatment with alkaline phosphatase conjugated secondary antibody. The sections were visualized with fast red. No counterstain was applied.

Omission or substitution of the primary antibody with an irrelevant antibody from the same species (rabbit monoclonal anti-human estrogen receptor α; ready-to-use; clone EPI, Dako) and staining with chromogen alone were used as negative controls.

Statistical analysis

Data are presented as the mean ± standard deviation. The non-parametric Mann-Whitney test was used to compare means from two independent groups. The Chi-square test was used for comparing proportions when analyzing data for two categorical variables. Pearson correlation coefficients were computed to investigate correlation between variables. A p-value less than 0.05 indicated statistical significance. SPSS version 20.0 for Windows (IBM Inc., Chicago, IL, USA) was used for statistical analysis.

Results

ELISA levels of thrombin, MMP-1 and VEGF in vitreous samples

With the use of ELISA, we demonstrated that thrombin was detected in all vitreous samples from patients with PDR and nondiabetic control patients. The mean thrombin level in vitreous samples from PDR patients (7.7±3.0 ng/ml) was significantly higher than the mean level in nondiabetic control patients (4.9±4.0 ng/ml) ($p=0.012$; Mann-Whitney test). MMP-1 was not detected in vitreous samples from nondiabetic control patients. However, MMP-1 was detected in 12 of 30 (40%) vitreous samples from patients with PDR. The mean MMP-1 level in vitreous samples from PDR patients (39.9±164.01 pg/ml) (range, 8-901 pg/ml) was significantly higher than the mean level in nondiabetic control patients ($p=0.002$; Mann-Whitney test). VEGF was detected in 11 of 22 (50%) vitreous samples from nondiabetic control patients, and in all vitreous samples from patients with PDR (n=24) ($p=0.0003$; Chi-square test). The mean VEGF level in vitreous samples from PDR patients (650.6±986.3 pg/ml) was significantly higher than that in nondiabetic control patients (25.6±59.9 pg/ml) ($p<0.0001$; Mann-Whitney test).

Correlations

Significant positive correlations were found between vitreous fluid levels of thrombin and levels of VEGF ($r=0.41$; $p=0.006$). A significant positive correlation was observed between vitreous fluid levels of MMP-1 and VEGF ($r=0.66$; $p<0.0001$) (Fig. 1). In contrast, the correlation between vitreous fluid levels of thrombin and MMP-1 was not significant.

Western blot analysis of vitreous samples

With the use of Western blot analysis of equal volumes (15 μL) of vitreous samples, we confirmed that thrombin and MMP-1 were expressed in vitreous samples. Thrombin protein migrated as two protein bands on SDS-PAGE when immunoblotted and analyzed with the specific antibody. The upper band corresponded to the zymogen prothrombin (approximately 70 kDa), whereas the lower protein band corresponded to the proteolytically active thrombin (approximately 50 kDa) (Fig. 2A). When MMP-1 was analyzed by Western blot, we observed that MMP-1 protein migrated as two protein bands at approximately 60 kDa (proMMP-1) and approximately 50 kDa (activated form of MMP-1) (Fig 2B).

Immunohistochemical analysis of epiretinal membranes

To identify the cell types expressing PAR1, epiretinal membranes from patients with PDR were studied by immunohistochemical analysis. No staining was observed in the negative control slides (Fig. 3A). All membranes showed blood vessels that were positive for the endothelial cell marker CD31 (Fig. 3B). Strong immunoreactivity for PAR1 was present in all membranes and was noted in vascular endothelial cells, stromal cells and intravascular leukocytes (Fig. 3C, D, E). In serial sections, the distribution and morphology of stromal cells expressing PAR1 were similar to those of cells expressing the leukocyte common antigen CD45 (Fig. 3F). In addition, the distribution and morphology of spindle-shaped stromal cells expressing PAR1 (Fig. 3E) were similar to those of spindle-shaped stromal cells expressing the myofibroblast marker α-SMA (Fig. 3G). Double staining confirmed that stromal leukocytes and intravascular leukocytes expressing PAR1 co-expressed CD45 (Fig. 3H).

The proinflammatory cytokines IL-1β and TNF-α, but not high-glucose and the hypoxia mimetic agents $CoCl_2$ induce upregulation of PAR1 in HRMEC.

To confirm the observed expression of PAR1 by endothelial cells, we performed induction experiments on HRMEC with inducers relevant in the context of PDR such as high-glucose, proinflammatory cytokines and hypoxia. Thus, we treated the HRMEC either with 30 mM glucose or 30 mM mannitol for 72 hours or for 24 hours with 10 ng/ml IL-1β, 30 ng/ml TNF-α, IL-1β plus TNF-α or 100 μM $CoCl_2$ and compared the levels of expression of PAR1 in whole cell extracts by Western blot analysis.

PAR1 protein migrated as three prominent protein bands on SDS-PAGE when immunoblotted and analyzed with specific antibody. The upper band corresponded to the intact protein (approximately 65 kDa), whereas the lower protein bands corresponded to cleaved PAR1 (approximately 50 kDa and 30 kDa). Densitometric analysis of the bands demonstrated a significant increase in the 30-kDa fragment expression and in the ratios of the 30-kDa fragment over the full length protein in response to IL-1β, TNF-α or IL-1β plus TNF-α. In contrast, the expression of the full length protein (approximately 65 kDa) and the 50-kDa fragment did not change (Fig. 4). Treatment of HRMEC with high-glucose and $CoCl_2$ did not affect the expression of PAR1 as compared to untreated control (data not shown).

Severity of hyperglycemia and effect of diabetes on retinal expression of PAR1 and thrombin in experimental rats

To validate our observations and to obtain a better view of the studied molecules in the pathogenesis of diabetic retinopathy, we used a rat animal model. After induction of diabetes with a single high-dose of streptozotocin, the body weights of the diabetic rats were significantly lower and their blood glucose values were more than four-fold higher compared with age-matched normal control rats (164 ± 28 versus 297 ± 19 g and 458 ± 24 versus 107 ± 14 mg/dl, respectively). Western blot analysis of homogenized retinal tissue demonstrated that PAR1 protein migrated as two protein bands at approximately 65 kDa and 50 kDa. Thrombin protein migrated as two protein bands at approximately 70 kDa and 50 kDa. Densitometric analysis of the bands demonstrated that the ratios of the cleaved PAR 1 (approximately 50 kDa) over the intact protein (approximately 65 kDa) and of the proteolytically active thrombin (approximately 50 kDa) over the zymogen prothrombin (approximately 70 kDa) were significantly higher in the retinas of diabetic rats compared to the retinas of nondiabetic control rats (n=7) (Fig. 5).

Thrombin and MMP-1 induce upgregulation of VEGF in HRMEC

To confirm the significant positive correlation between the vitreous fluid levels of thrombin and MMP-1 with those of the angiogenic biomarker VEGF, we performed induction experiments on HRMEC with thrombin and MMP-1. HRMEC were stimulated for 24 hours with 1nM rh thrombin or 5nM rh MMP-1, and we compared the levels of expression of VEGF in the whole cell extracts by Western blot analysis. We found that both thrombin and MMP-1 treatments significantly increased the expression of VEGF (Fig. 6). Vorapaxar pre-treatment did not inhibit upregulation of VEGF induced by thrombin (data not shown).

The PAR1 inhibitor vorapaxar inhibits thrombin-induced migration in HRMEC

Next we tested the effect of PAR1 on thrombin-induced *in vitro* migration in HRMEC. For this purpose, we used the specific PAR1 inhibitor vorapaxar. HRMEC were left untreated or treated either with thrombin or with vorapaxar for 30 minutes before addition of thrombin and *in vitro* migration was analyzed. Our data convincingly showed that vorapaxar pre-treatment significantly inhibited the migration induced by thrombin in HRMEC (Fig. 7). These results provided evidence that PAR1 signaling is involved in the migration induced by thrombin in HRMEC. On the other hand, MMP-1 did not induce migration in HRMEC (Fig. 7).

Discussion

Activation of PAR1 signaling in endothelial cells induces both their proliferation and recruitment and promotes angiogenesis by increasing the expression, activation and secretion of angiogenic growth factors such as VEGF [10, 15]. The expression of PAR1 in tumor cells is sufficient to induce functional VEGF expression levels, eliciting tumor angiogenesis both *in vivo* in animal models and *in vitro* (as shown by the endothelial tube forming assay and cell migration) [17, 18]. In addition, PAR1 is required in endothelial cells for maturation and stabilization of the blood vessels [17]. Inhibition of PAR1 resulted in decreased expression of VEGF and decreased blood vessel density in melanoma tumors [10].

In the present study, we investigated this signaling cascade in diabetic retinopathy and showed, for the first time, that PAR1 immunoreactivity was specifically localized in vascular endothelial cells, leukocytes expressing the leukocyte common antigen CD45, and myofibroblasts in epiretinal fibrovascular membranes from patients with PDR. Our data are in line of those of others, who have shown that PAR1 is expressed by a variety of cell types in the tumor microenvironment, including endothelial cells, platelets, macrophages, and fibroblasts [10]. Furthermore, we showed that cleaved PAR1 (approximately 50 kDa) was significantly upregulated in the retinas of diabetic rats. To corroborate the findings at the cellular level, stimulation with the proinflammatory cytokines IL-Iβ and TNF-α caused upregulation of cleaved PAR1 (approximately 30 kDa) in HRMEC. On the other hand, high-glucose and the hypoxia mimetic agent $CoCl_2$ did not affect the expression of PAR1 in HRMEC. Taken together, these findings suggest that inflammation, but not hyperglycemia and hypoxia might be involved in diabetes-induced PAR1 upregulation, which might be a chief pathophysiologic mechanism for diabetic retinopathy. It was demonstrated that cleavage of PAR1 reveals a new amino terminus domain that functions as a tethered ligand by binding to its receptor and initiates downstream signaling [10-12]. These findings are consistent with previous studies that demonstrated upregulation of PAR1 in the kidney of diabetic mice [20], and that advanced glycation end-products, thought to play a pivotal role in the pathogenesis of diabetic retinopathy [21], increase PAR1 expression in endothelial cells [22]. Taken together, these findings suggest that diabetes-induced retinal endothelial structural damage leads to their proliferation and sprouting by inducing PAR1 expression, which might be a chief pathophysiologic mechanism in PDR.

Thrombin is a serine protease that is generated from its inactive precursor prothrombin. In addition to its central role in the coagulation cascade via platelet activation and fibrin deposition, thrombin is a key supporter of various cellular effects, relevant for tumor growth and metastasis, as well as a potent activator of angiogenesis. The main mechanism responsible for these cellular actions of thrombin is mediated by PAR1 which has been shown to respond with high affinity to thrombin [12, 23, 24]. Angiogenesis involves the activation and invasion of endothelial cells through their basement membrane, proliferation and migration to distal sites. It has been demonstrated that thrombin contributes to each of these events through PAR1 signaling [12, 24] and that PAR1 antagonists are very potent anti-angiogenic agents [12]. In addition, thrombin has a potent anti-apoptotic effect on serum-starved endothelial cells [25]. Several vascular regulatory proteins and growth factors have been shown to be activated or upregulated by thrombin. For example, thrombin-induced angiogenesis is associated with upregulation of VEGF. Thrombin increased VEGF levels in several cell types, such as endothelial cells and it induced VEGF receptor-2 expression in endothelial cells. Another important effect of thrombin is the potentiation of the mitogenic activity of VEGF on endothelial cells [12, 15, 23-26].

In the present study, we showed for the first time that a procoagulant condition is created in the eye by diabetes, because thrombin was significantly upregulated in the vitreous fluid from patients with PDR and in the retinas of diabetic rats. In addition, we found a significant positive correlation between the vitreous fluid levels of thrombin and those of the angiogenic biomarker VEGF, a key angiogenic factor in PDR [4], and that stimulation with thrombin caused upregulation of VEGF in HRMEC. It should be emphasized that thrombin and VEGF were detected in all and 50%, respectively, of vitreous samples from patients with rhegmatogenous retinal detachment with no proliferative vitreoretinopathy. These findings are consistent with previous reports that demonstrated upregulated expression of inflammatory mediators in the vitreous fluid from patients with rhegmatogenous retinal detachment [27-29] and in the detached retina following experimental retinal detachment [30]. The present findings are consistent with previous studies that demonstrated active involvement of thrombin in the upregulation of VEGF expression in several cell lines [12, 15, 23-26]. The results of the present study also show that vorapaxar, a potent PAR1 receptor antagonist [19], inhibited HRMEC migration, a key early step in angiogenesis, induced by thrombin. Together, these results provide evidence that thrombin and its receptor PAR1 might mediate angiogenesis in PDR. Furthermore, several studies demonstrated that thrombin activation mediates intracerebral hemorrhage-induced neurotoxicity and severe blood-brain barrier disruption and neuronal cell death during brain ischemia [31-34]. The direct cytotoxic effects of thrombin appear to be mediated by PAR1 [31, 32].

MMP-1 is an interstitial collagenase that is often upregulated in several types of cancer, and this enzyme is involved in tumor-induced angiogenesis [14, 35-38]. Purified MMP-1 is also capable of inducing angiogenesis *in vivo*, thereby defining MMP-1 as a pro-angiogenic factor [14]. Recently, Boire et al [13] showed that MMP-1 is an additional proteolytic activator of PAR1, promoting angiogenesis, invasion and tumorigenesis of cancer cells *in vitro* and *in vivo.* The pro-angiogenic effects of MMP-1 are significantly reduced when PAR1 activation is inhibited [13, 14]. Further, activation of endothelial cells by MMP-1 [14], and of cancer cells [16] via PAR1 induces the secretion of several angiogenic factors. Furthermore, the combination of thrombin and MMP-1 is more angiogenic than either protease alone [14]. In addition, tumor-derived MMP-1 activates endothelial PAR1 to induce disruption of the vascular endothelial barrier and increases vascular permeability [39], a characteristic sign of diabetic retinopathy [40]. In the current study, we found that MMP-1 was significantly upregulated in the vitreous fluid from patients with PDR and that there was a significant positive correlation between the levels of MMP-1 and VEGF. To corroborate the findings at the cellular level, stimulation with MMP-1 caused upregulation of VEGF in HRMEC.

In conclusion, our data provide evidence that PAR1, thrombin and MMP-1 are expressed within the ocular microenvironment of patients with PDR and show that PAR1 and thrombin might facilitate angiogenesis and progression of PDR by inducing endothelial cell migration, as well as secretion of angiogenic mediators. These findings suggest that this signaling axis may present a new avenue for therapeutic intervention in patients with diabetic retinopathy.

Acknowledgments

The authors thank Ms. Connie B. Unisa-Marfil for secretarial work; Mr. Wilfried Versin and Ms. Nathalie Volders for technical assistance. This work was supported by Dr. Nasser Al-Rashid Research Chair in Ophthalmology (Abu El-Asrar AM).

.

Declaration of Interest

All the authors do not have any conflict of interests with any trademark mentioned in the manuscript. The authors alone are responsible for the content and writing of the paper.

References

1. Carmeliet P. Angiogenesis in health and disease. Nat Med 2003; 9:653-60.
2. Nierodzik ML, Karpatkin S. Thrombin induces tumor growth, metastasis, and angiogenesis: Evidence for a thrombin-regulated dormant tumor phenotype. Cancer Cell 2006; 10:355-62.
3. Hanahan D, Folkman J. Patterns and emerging mechanisms of the angiogenic switch during tumorigenesis. Cell 1996; 86:353-64.
4. Spranger J, Pfeiffer AP. New concepts in pathogenesis and treatment of diabetic retinopathy. Exp Clin Endocrinol Diabetes 2001; 109:S438-50.
5. Joussen AM, Poulaki V, Le ML, Koizumi K, Esser C, Janicki H, et al. A central role for inflammation in the pathogenesis of diabetic retinopathy. FASEB J 2004; 18:1450-2.
6. Kaji Y, Usui T, Ishida S, Yamashiro K, Moore TC, Moore J, et al. Inhibition of diabetic leukostasis and blood-retinal barrier breakdown with a soluble form of a receptor for advanced glycation end products. Invest Ophthalmol Vis Sci 2007; 48:858-65.
7. Li G, Tang J, Du Y, Lee CA, Kern TS. Beneficial effects of novel RAGE inhibitor on early diabetic retinopathy and tactile allodynia. Mol Vis 2011; 17:3156-65.
8. Costa C, Incio J, Soares R. Angiogenesis and chronic inflammation: cause or consequence? Angiogenesis 2007; 10:149-66.
9. Salam A, Mathew R, Sivaprasad S. Treatment of proliferative diabetic retinopathy with anti-VEGF agents. Acta Ophthalmol 2011; 89:405-11.
10. Zigler M, Kamiya T, Brantley EC, Villares GJ, Bar-Eli M. PAR-1 and thrombin: The ties that bind the microenvironment to melanoma metastasis. Cancer Res 2011; 71:6561-6.
11. Austin KM, Covic L, Kuliopulos A. Matrix metalloproteases and PAR1 activation. Blood 2013; 121:431-9.
12. Tsopanoglou NE, Maragoudakis ME. Thrombin's central role in angiogenesis and pathophysiological processes. Eur Cytokine Netw 2009; 20:171-9.

13. Boire A, Covic L, Agarwal A, Jacques S, Sherifi S, Kuliopulos A. PAR1 is a matrix metalloprotease-1 receptor that promotes invasion and tumorigenesis of breast cancer cells. Cell 2005;120:303-13.
14. Blackburn JS, Brinckerhoff CE. Matrix metalloproteinase-1 and thrombin differentially activate gene expression in endothelial cells via PAR-1 and promote angiogenesis. Am J Pathol 2008;173:1736-46.
15. Tsopanoglou NE, Maragoudakis ME. Inhibition of angiogenesis by small-molecule antagonists of protease-activated receptor-1. Semin Thromb Hemost 2007; 33:680-7.
16. Agarwal A, Tressel SL, Kaimal R, Balla M, Lam FH, Covic L, et al. Identification of a metalloprotease-chemokine signaling system in the ovarian cancer microenvironment: Implications for antiangiogenic therapy. Cancer Res 2010; 70:5880-90.
17. Yin YJ, Salah Z, Maoz M, Ram SCE, Ochayon S, Neufeld G, et al. Oncogenic transformation induces tumor angiogenesis: a role for PAR1 activation. FASEB J 2003; 17:163-74.
18. Agarwal A, Covic L, Sevigny LM, Kaneider NC, Lazarides K, Azabdaftari G, et al. Targeting a metalloprotease-PAR1 signaling system with cell-penetrating pepducins inhibits angiogenesis, ascites, and progression of ovarian cancer. Mol Cancer Ther 2008; 7:2746-57.
19. Cho JR, Rollini F, Franchi F, Ferrante E, Angiolillo DJ. Unmet needs in the management of acute myocardial infarction: role of novel protease-activated receptor-1 antagonist vorapaxar. Vasc Health Risk Manag 2014; 10:177-88.
20. Sakai T, Nambu T, Katoh M, Uehara S, Fukuroda T, Nishikibe M. Up-regulation of protease-activated receptor-1 in diabetic glomerulosclerosis. Biochem Biophys Res Commun 2009; 384:173-9.
21. Chen M, Curtis TM, Stitt AW. Advanced glycation end products and diabetic retinopathy. Curr Med Chem 2013; 20:3234-40.
22. Ishibashi Y, Matsui T, Ueda S, Fukami K, Yamagishi S. Advanced glycation end products potentiate citrated plasma-evoked oxidative and inflammatory reactions in endothelial cells by up-regulating protease-activated receptor-1 expression. Cardiovasc Diabetol. 2014 doi: 10.1186/1475-2840-13-60.
23. Liu J, Schuff-Werner P, Steiner M. Thrombin/thrombin receptor (PAR-1)-mediated induction of IL-8 and VEGF expression in prostate cancer cells. Biochem Biophys Res Comm 2006; 343:183-9.
24. Han N, Jin K, He K, Cao J, Teng L. Protease-activated receptors in cancer: A systematic review. Oncology Letters 2011; 2:599-608.
25. Zania P, Papaconstantinou M, Flordellis CS, Maragoudakis ME, Tsopanoglou NE. Thrombin mediates mitogenesis and survival of human endothelial cells through distinct mechanisms. Am J Physiol Cell Physiol 2008; 294:C1215-26.
26. Nierodzik ML, Karpatkin S. Thrombin induces tumor growth, metastasis, and angiogenesis: Evidence for a thrombin-regulated dormant tumor phenotype. Cancer Cell 2006; 10:355-62.
27. Dai Y, Wu Z, Sheng H, Zhang Z, Yu M, zhang Q. Identification of inflammatory mediators in patients with rhegmatogenous retinal detachment associated with choroidal detachment. Mol Vis 2015; 21:417-427.
28. Yoshimura T, Sonoda KH, Sugahara M, Mochizaki Y, Enaida H, Oshima Y, et al. Comprehensive analysis of inflammatory immune mediators in vitreoretinal diseases. PLoS One 2009; 4(12):e8158.
29. Abu El-Asrar AM, Van Damme J, Put W, Veckeneer M, Dralands L, Billiau A, et al. Monocyte chemotactic protein-1 in proliferative vitreoretinal disorders. Am J Ophthalmol 1997; 123:599-606.

30. Nakazawa T, Matsubara A, Noda K, Hisatomi T, She H, Skondra D, et al. Characterization of cytokine responses to retinal detachment in rats. Mol Vis. 2006;12:867-878.
31. Xue M, Hollenberg MD, Yong VW. Combination of thrombin and matrix metalloproteinase-9 exacerbates neurotoxicity in cell culture and intracerebral hemorrhage in mice. J Neurosci 2006; 26:10281-91.
32. Xue M, Hollenberg MD, Demchuk A, Yong VW. Relative importance of proteinase-activated receptor-1 versus matrix metalloproteinases in intracerebral hemorrhage-mediated nerurotoxicity in mice. Stroke 2009; 40:2199-204.
33. Xue M, Fan Y, Liu S, Zygun DA, Demchuk A, Yong VW. Contributions of multiple proteases to neurotoxicity in a mouse model of intracerebral haemorrhage. Brain 2009; 132:26-36.
34. Chen B, Cheng Q, Yang K, Lyden PD. Thrombin mediates severe neurovascular injury during ischemia. Stroke 2010; 41:2348-52.
35. Pulukuri SM, Rao JS. Matrix metalloproteinase-1 promotes prostate tumor growth and metastasis. Int J Oncol 2008; 32:757-65.
36. Goerge T, Barg A, Schnaeker EM, Poppelmann B, Shpacovitch V, Rattenholl A, et al. Tumor-derived matrix metalloproteinase-1 targets endothelial proteinase-activated receptor 1 promoting endothelial cell activation. Cancer Res 2006; 66:7766-74.
37. Blackburn JS, Rhodes CH, Coon CI, Brinckerhoff CE. RNA interference inhibition of matrix metalloproteinase-1 prevents melanoma metastasis by reducing tumor collagenase activity and angiogenesis. Cancer Res 2007; 67:10849-58.
38. Eck SM, Hoopes PJ, Petrella BL, Coon CI, Brinckerhoff CE. Matrix metalloproteinase-1 promotes breast cancer angiogenesis and osteolysis in a novel in vivo model. Breast Cancer Res Treat 2009; 116:79-90.
39. Juncker-Jensen A, Deryugina E, Rimann I, Zajac E, Kupriyanova TA, Engelholm LH, et al. Tumor MMP-1 activates endothelial PAR1 to facilitate vascular intravasation and metastatic dissemination. Cancer Res 2013; 73:4196-211.
40. Ferris FL 3rd, Patz A. Macular edema. A complication of diabetic retinopathy. Surv Ophthalmol 1984; 28 Suppl:452-61.

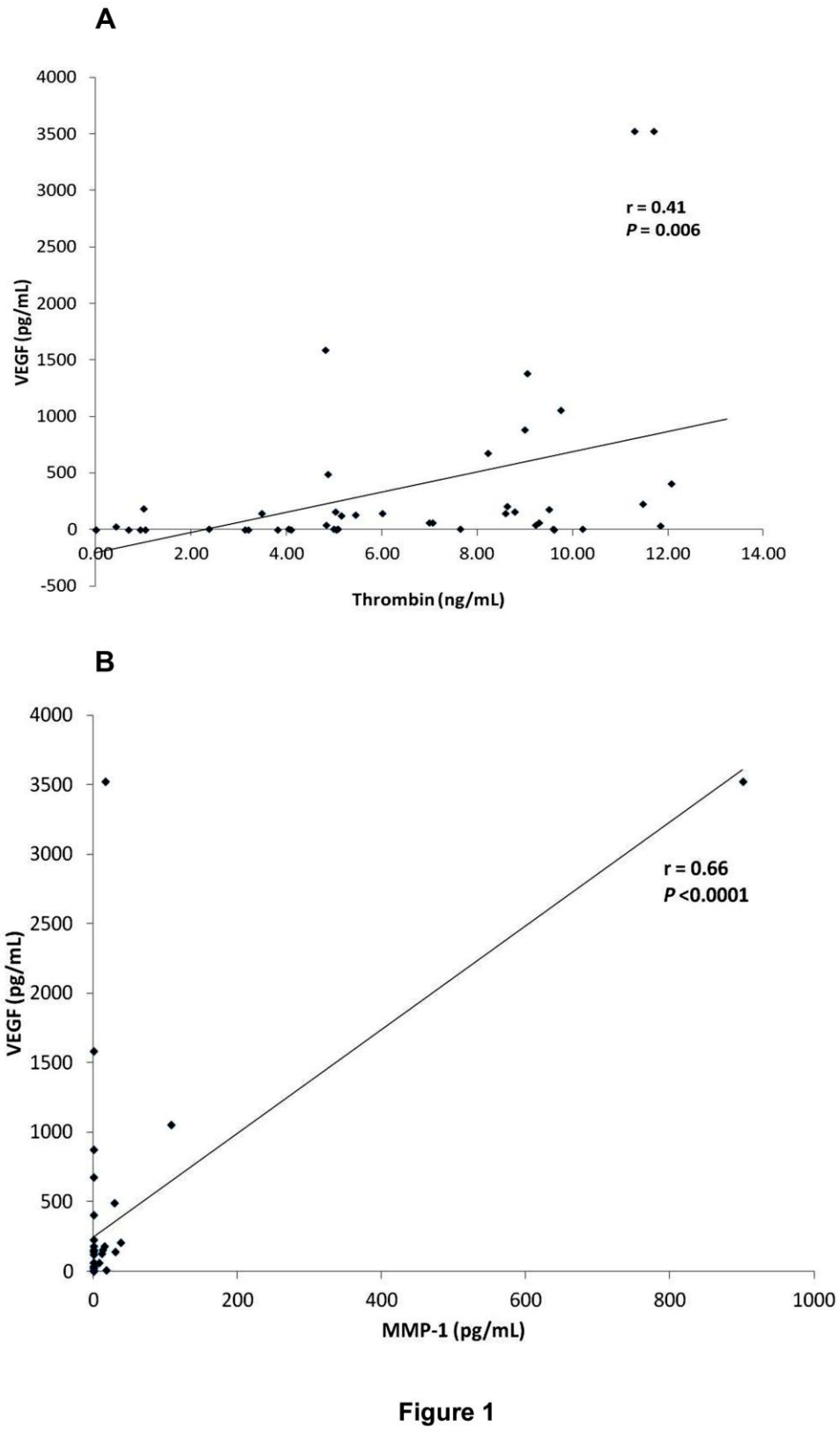

Figure 1. Significant positive correlations between vitreous fluid levels of thrombin and the levels of vascular endothelial growth factor (VEGF) (A) and between the vitreous fluid levels of MMP-1 and the levels of VEGF (B).

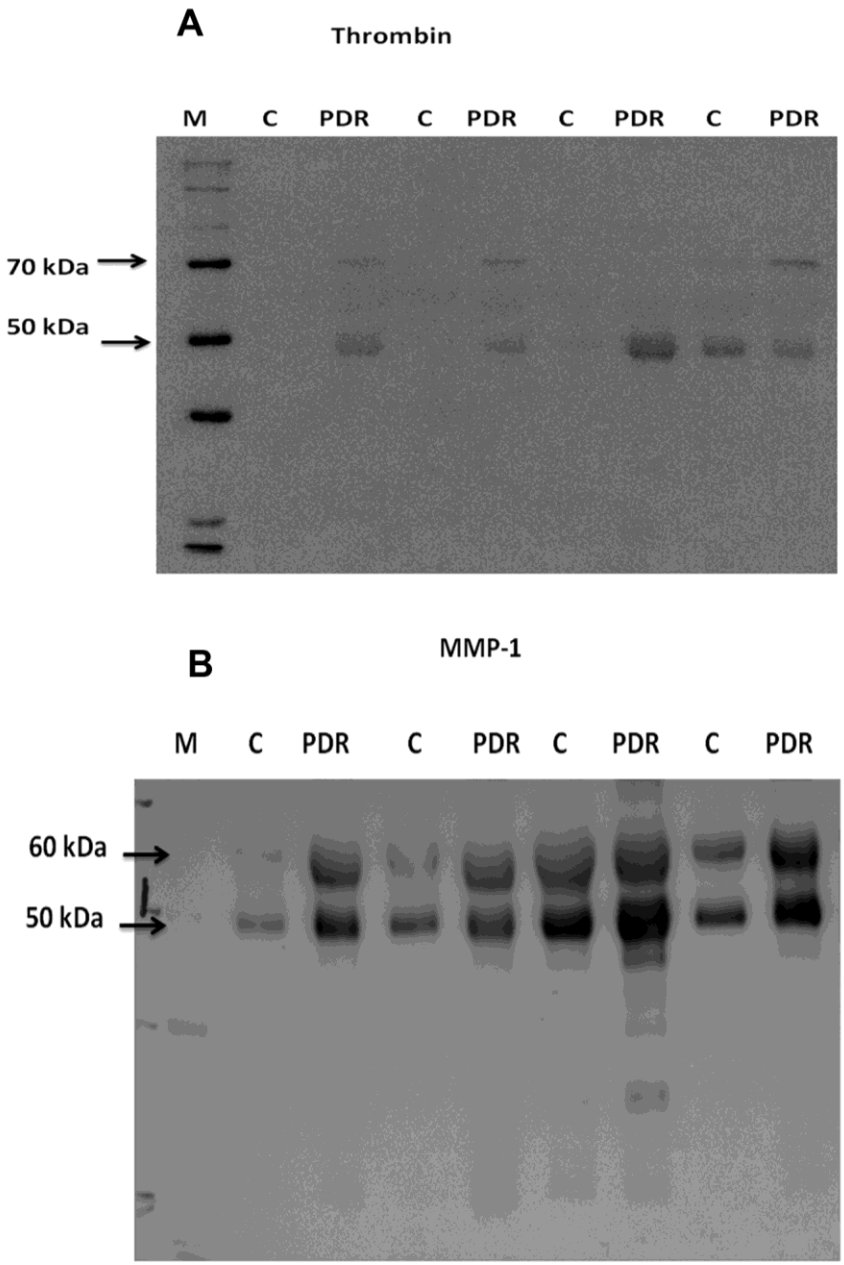

Figure 2

Figure 2. The expressions of thrombin (A) and matrix metalloproteinase-1 (MMP-1) (B) in equal volumes (15 μL) of vitreous samples from patients with proliferative diabetic retinopathy (PDR) and from control patients without diabetes (C) were determined by Western blot analysis. Thrombin protein migrated as two protein bands on SDS-PAGE when immunoblotted and analyzed with the specific antibody. The upper band corresponded to the zymogen prothrombin (approximately 70 kDa), whereas the lower protein band corresponded to the proteolytically active thrombin (approximately 50 kDa). MMP-1 protein migrated as two protein bands at approximately 60 kDa (proMMP-1) and approximately 50 kDa (activated MMP-1) Representative set of samples are shown.

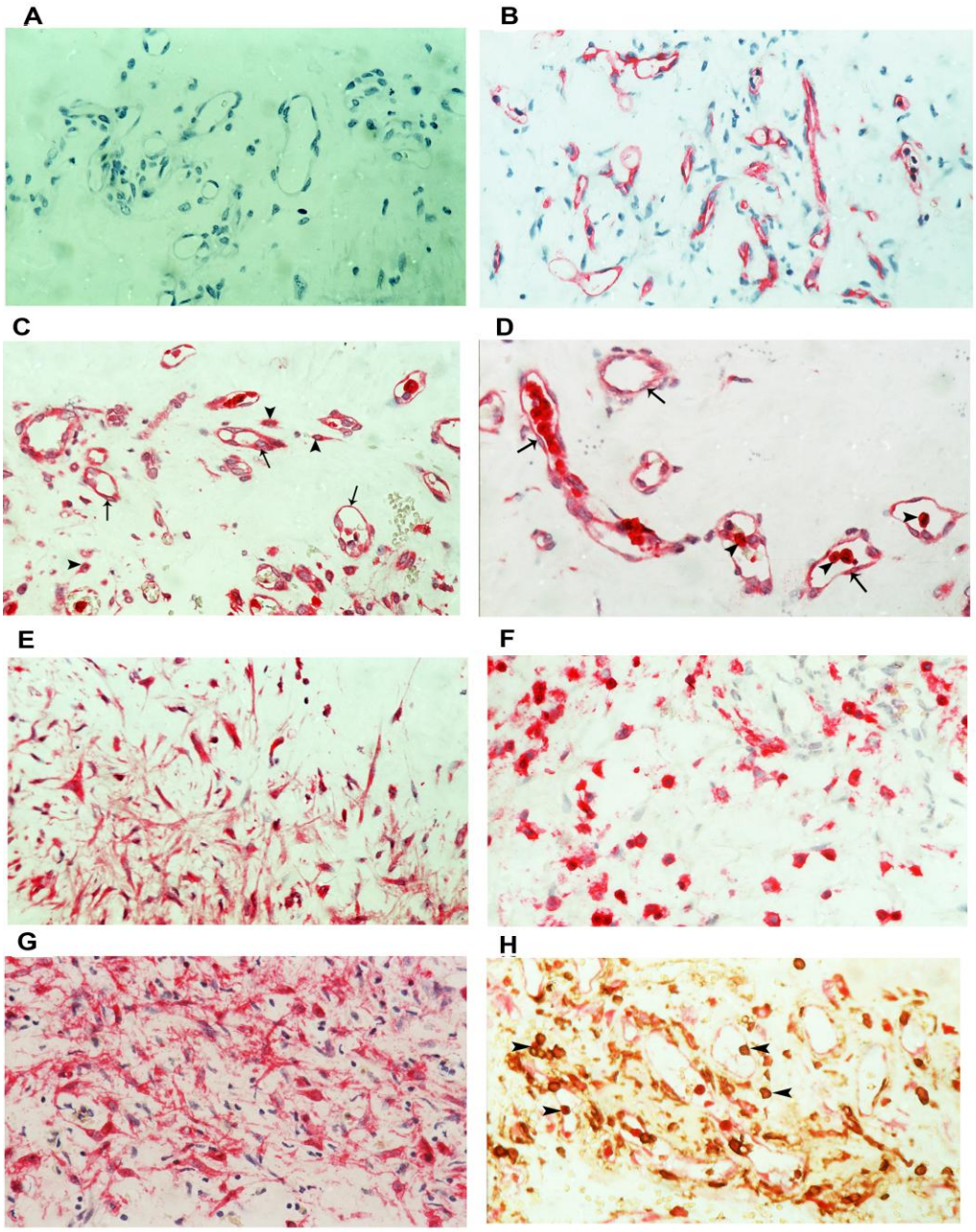

Figure 3. Proliferative diabetic retinopathy epiretinal membranes. Negative control slide that was treated identically with an irrelevant antibody showing no labeling (A). Immunohistochemical staining for CD31 showing blood vessels positive for CD31 (B). Immunohistochemical staining for protease-activated receptor-1 (PAR1) showing immunoreactivity in the vascular endothelium (arrows), in stromal cells (arrowheads) (C), in intravascular leukocytes (arrowheads) (D) and in stromal spindle-shaped cells (E). Immunohistochemical staining for CD45 showing stromal cells positive for CD45 (F). Immunohistochemical staining for α-smooth muscle actin showing immunoreactivity in spindle-shaped myofibroblasts (G). Double immunohistochemistry for CD45 (brown) and PAR1 (red) showing stromal cells and intravascular leukocytes (arrowheads) co-expressing CD45 and PAR1 (H) (original magnification X40).

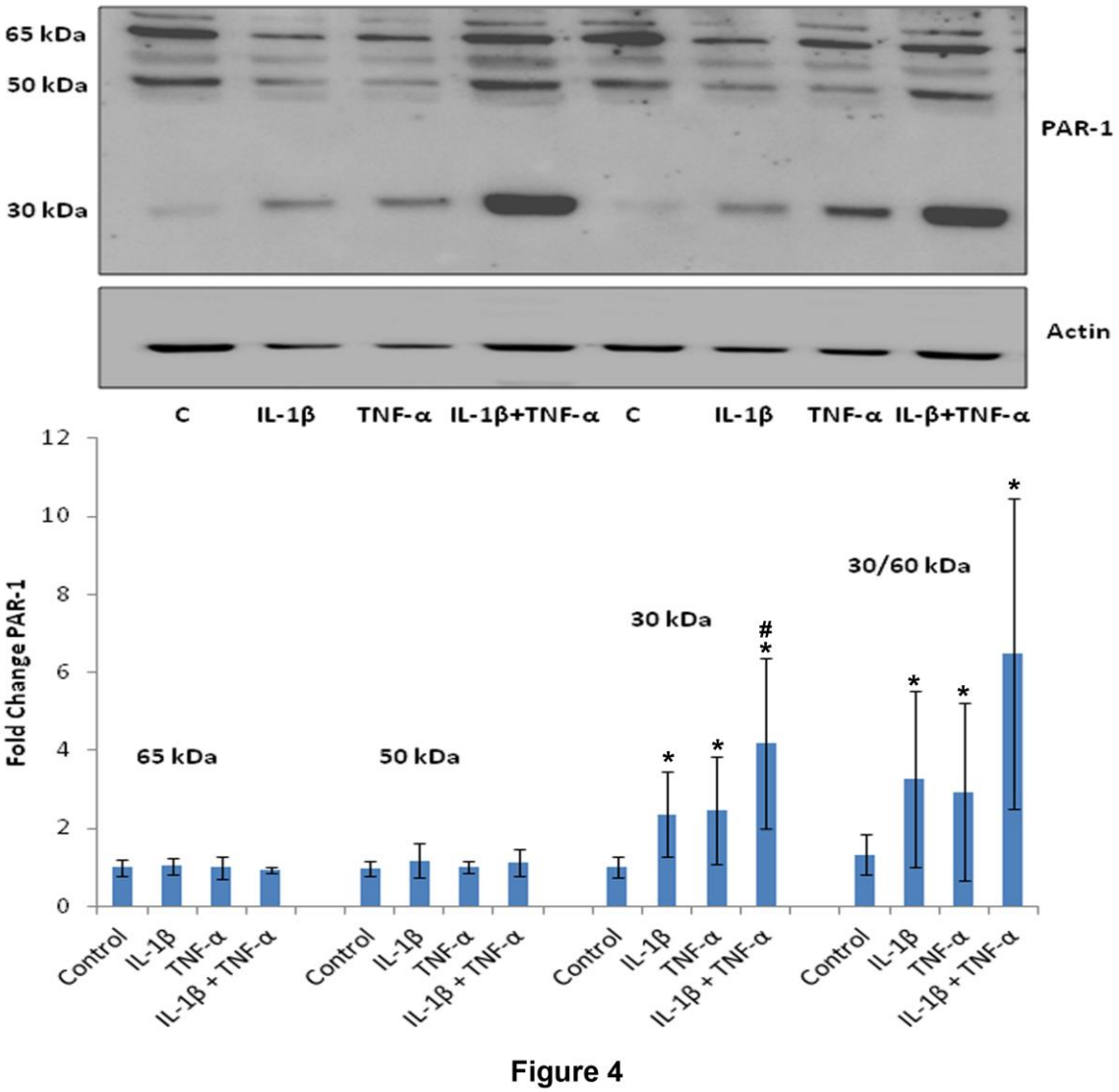

Figure 4

Figure 4. Human retinal microvascular endothelial cells were left untreated or were treated with either IL-1β (10 ng/ml), TNF-α (30 ng/ml), or with a combination of cytokines containing IL-1β (10 ng/ml) plus TNF-α (30 ng/ml) for 24 hours. The levels of expression of protease-activated receptor-1 (PAR1) were compared by Western blot analysis. Western blots are representative of at least three independent experiments, each is performed in duplicate and bar graphs are representative of all three experiments. *P <0.05 compared to untreated control. $^{\#}$P <0.05 compared to IL-1β.

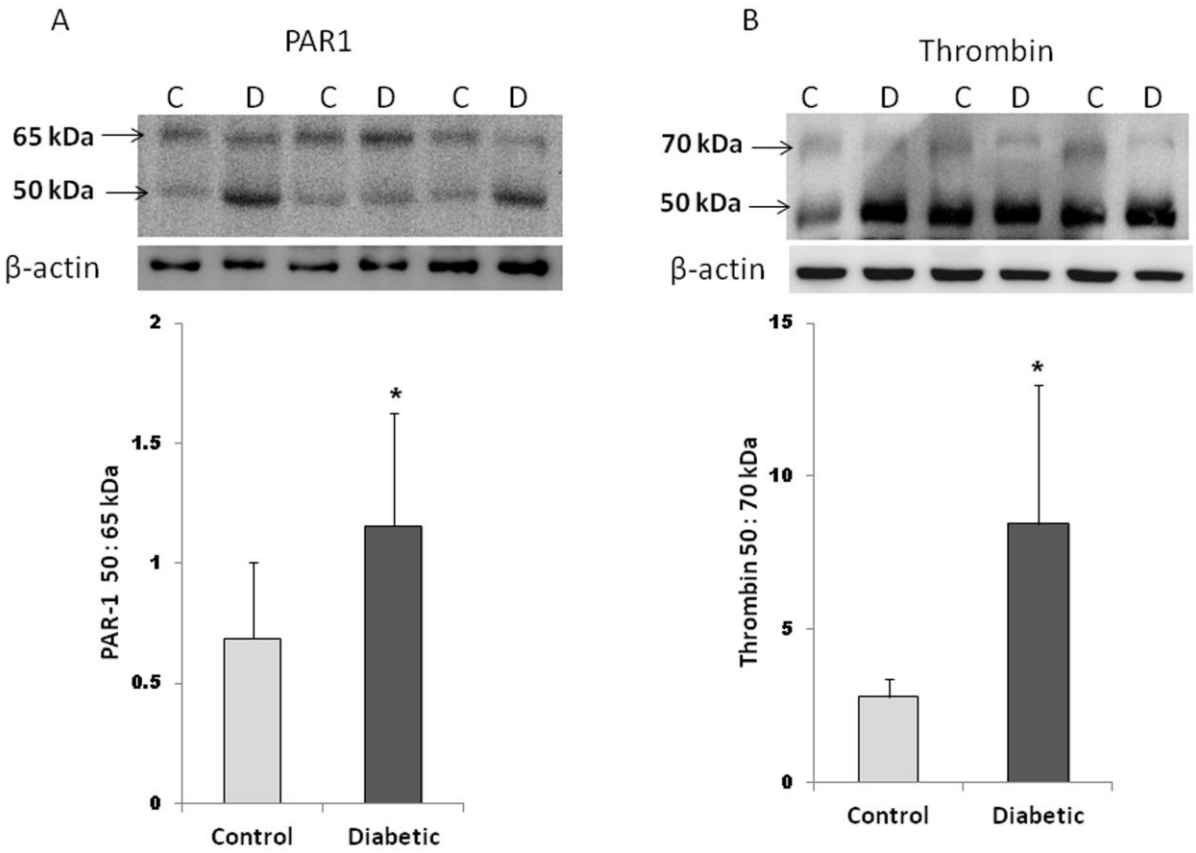

Figure 5

Figure 5. Western blot analysis of protease-activated receptor-1 (PAR1) (A) and thrombin (B) in rat retinas. Significant increases in the ratios of the cleaved PAR1 over the intact protein and of the proteolytically active thrombin over the zymogen prothrombin in the retinas of diabetic rats (D) compared to the nondiabetic control rats (C). Each experiment was repeated 3 times with fresh samples (n=7). *P <0.05 compared to control.

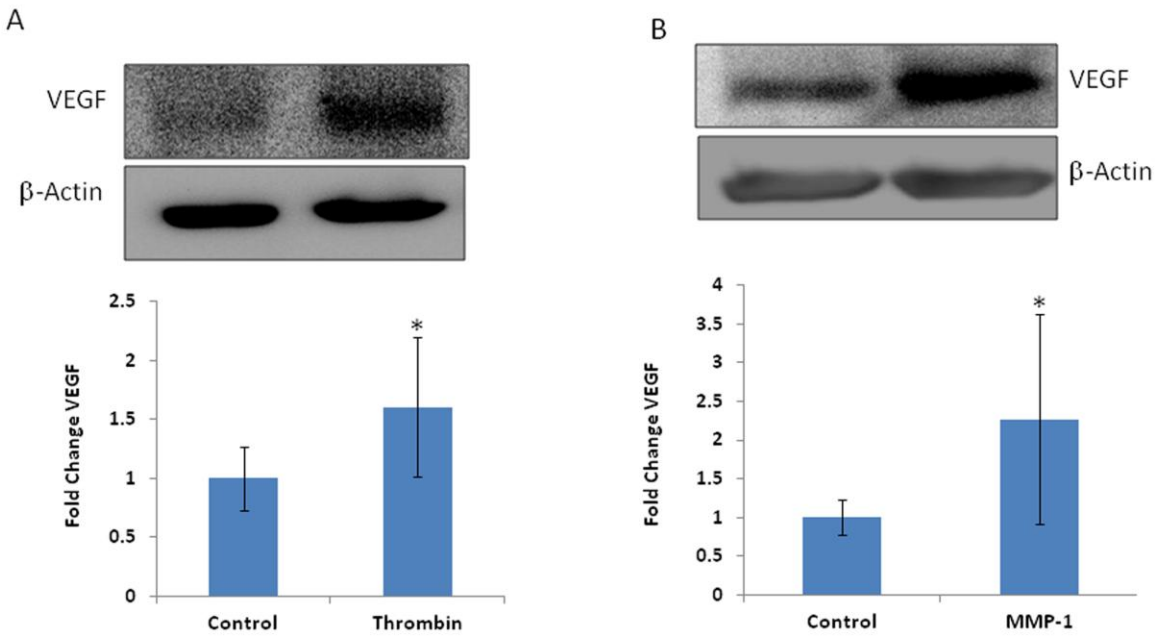

Figure 6

Figure 6. Effects of thrombin (A) and matrix metalloproteinase-1 (MMP-1) (B) on the expression of vascular endothelial growth factor (VEGF) in human retinal microvascular endothelial cells. Protein expression of VEGF in treated and untreated (control) cell lysates was determined by Western blot analysis. Western blots are representative of at least three independent experiments, each is performed in duplicate and bar graphs are representative of all three experiments. *P <0.05 compared to untreated control.

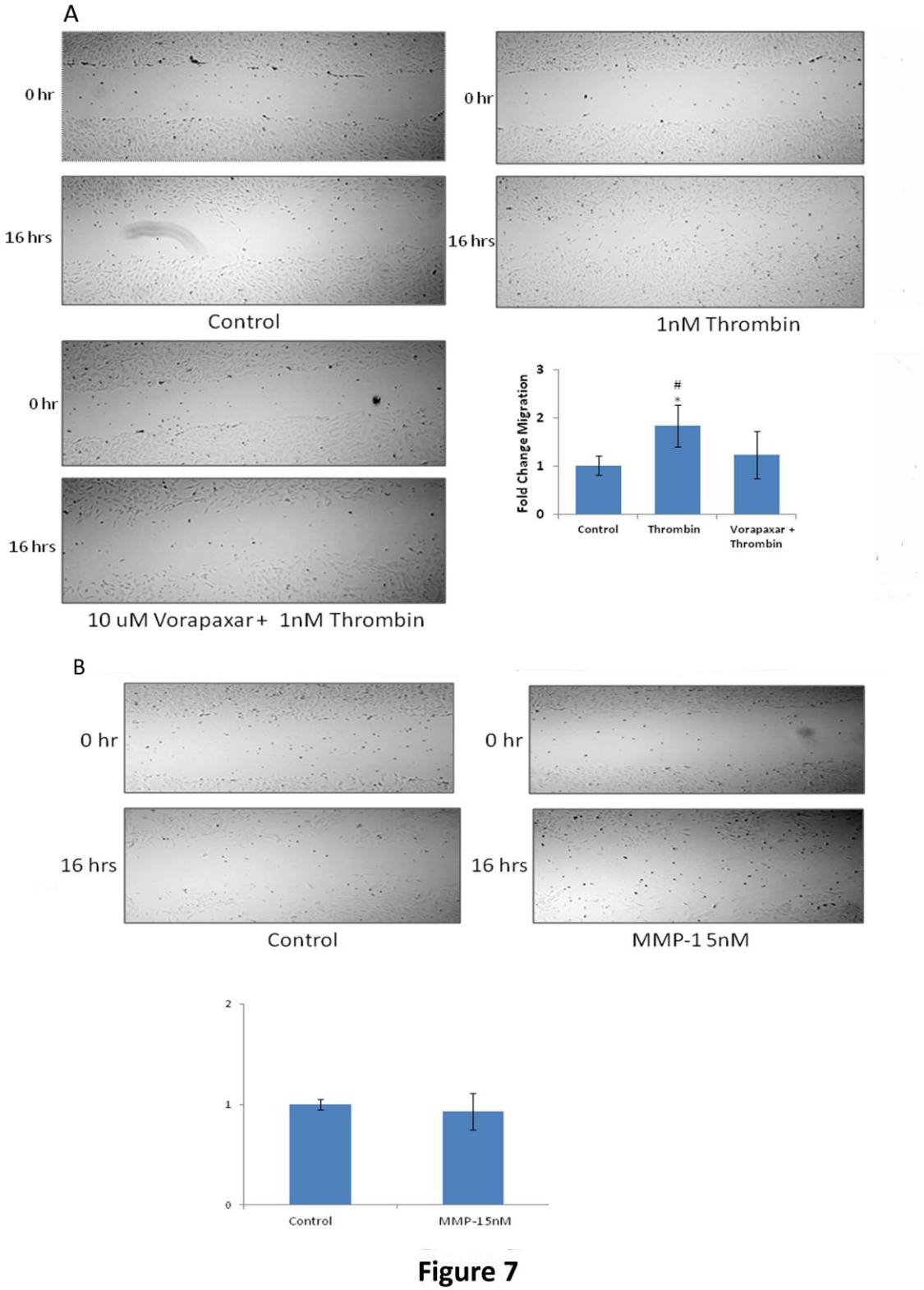

Figure 7

Figure 7. Effects of thrombin (A) and matrix metalloproteinase -1 (MMP-1) (B) on migration of human retinal microvascular endothelial cells (HRMEC). Thrombin-induced migration of HRMEC was inhibited by the protease-activated receptor-1 (PAR1) inhibitor vorapaxar. HMREC were left untreated or treated either with 1nM

recombinant thrombin, with 10 μM PAR1 inhibitor vorapaxar for 30 minutes before addition of 1nM recombinant thrombin or with 5 nM recombinant MMP-1. Cells were visualized using inverted microscope (Olympus 1X 81, Olympus Corporation, Tokyo, Japan). Three independent experiments were performed. Six independent field images were taken from each treated group for migration analysis which was done by using Image J software. One image from each group is illustrated and the bar graphs show the analysis of all six images from each group. *P <0.05 compared to untreated control. $^{\#}$P <0.05 compared to vorapaxar + thrombin.